Relativistic mean-field model for the ultracompact low-mass neutron star HESS J1731-347

Sebastian Kubis [1,*] Włodzimierz Wójcik [1] David Alvarez Castillo [2] and Noemi Zabari [3]
[1]*Department of Physics, Cracow University of Technology, Podchorążych 1, 30-084 Kraków, Poland*
[2]*Henryk Niewodniczański Institute of Nuclear Physics, Polish Academy of Sciences, Radzikowskiego 152, 31-342 Kraków, Poland*
[3]*Astrotectonics, AstroTectonic Ltd., Słowackiego 24, 35-069 Rzeszów, Poland*

(Received 11 July 2023; accepted 5 October 2023; published 30 October 2023)

The recent observation of the object HESS J1731-347 suggests the existence of a very light and very compact neutron star, which is a challenge for commonly used equations of state for dense matter. In this work we present a relativistic mean-field model enriched with isovector and isoscalar meson crossing terms. These interactions dominate the behavior of the symmetry energy and account for the small radius. The proposed model fulfills the recent constraints concerning the symmetry energy slope and the state-of-the-art compact star constraints derived from the NICER measurements of the pulsars PSR J0030 + 0451 and PSR J0740 + 6620, as well as from the GW170817 event and its associated electromagnetic counterparts AT2017gfo/GRB170817A.

DOI: 10.1103/PhysRevC.108.045803

I. INTRODUCTION

The recent observation of a neutron star labeled as HESS J1731-347 [1] that has been identified as a very compact and light object challenges most of the state-of-the-art theoretical descriptions. To fulfill constraints from other observations, namely gravitational waves from GW170807 [2] and radio/x-ray detection of pulsars among others [3,4], realistic equations of state (EoSs) for compact stars tend to be stiff at higher densities (predicting more massive objects), whereas at lower densities they should be relatively soft. The characteristic feature of such EoSs is that the mass-radius relation has a Z-like shape with low-mass stars more compact than their high-mass counterparts. In this work we present a nuclear model capable of fulfilling all the recent observational constraints, including the inferred mass and radius values of HESS J1731-347.

HESS J1731-347 has been determined to be a very low-mass, small, compact star, associated with a supernova remnant. This is not the first time an object with such characteristics has been reported. However, in most other cases, corrections due to observations of radiating hot spots instead of the entire surface of the star had to be applied, resulting in larger stellar objects. One of the most important properties of compact stars featuring such surface spots is the signal pulsation. It is indeed the detections of x-ray pulsations produced by radiating spots that have allowed the NICER detector to derive estimates of the masses and radii of PSR J0030 + 0451 and PSR J0740 + 6620. The case of HESS J1731-347 has been reported as an exceptional central compact object (CCO), which is isolated, radio-quiet, and nonaccreting but thermally radiating. No pulsations were detected in its thermal emission, and its atmospheric composition has been determined to be mostly carbon. Moreover, the distance to this source, a very important quantity for electromagnetic flux determination, has been robustly derived from Gaia observations [5]. It would be honest to mention that despite many arguments supporting the low mass and compact size of the object, its unusual parameters are still a matter of debate, like for example in [6].

The very small stellar radius for light neutron stars considerably reduces the available parameter space for nuclear EoSs and highlights the potential of the HESS J1731-347 observation. The nuclear symmetry energy, whose stiffness is usually characterized by its slope-related parameter L, has a considerable impact on the compact star radius. The general trend is that larger L values result in larger stellar radii [7]. Here, we show that a small L around 40 MeV, being in agreement with the properties of nuclear matter, can make a compact size for HESS J1731-347.

In the next section, we introduce the pure hadronic relativistic mean-field (RMF) model with scalar-scalar and scalar-vector meson interactions and provide details of its properties. In the Results section, the important features of compact stars are discussed and compared to the recent observational data.

II. THE MODEL

In the RMF model, the interactions of nucleons are mediated by four types of mesons: σ, ω, ρ, and δ. The proposed Lagrangian $\mathcal{L}$ includes $\mathcal{L}_{\rm kin}$, the standard kinetic part for mesons and nucleons; $\mathcal{L}_{N\phi}$, Yukawa-type couplings of nucleons to mesons; $U(\sigma)$, the self-interaction term for σ; and $\mathcal{L}_{\rm cross}$, meson-meson interactions (crossing terms) between δ and σ and between δ and ω (further details are presented in [8]):

$$\mathcal{L} = \mathcal{L}_{\rm kin} + \mathcal{L}_{N\phi} - U(\sigma) + \mathcal{L}_{\rm cross}, \quad \phi = \sigma, \omega, \rho, \delta. \tag{1}$$

*skubis@pk.edu.pl

The most crucial ingredient is the crossing term

$$\mathcal{L}_{\text{cross}} = \tfrac{1}{2} g_{\sigma\delta}\, \sigma^2 \vec{\delta}^2 + \tfrac{1}{2} g_{\omega\delta}\, \omega_\mu \omega^\mu \vec{\delta}^2, \tag{2}$$

which represents quadratic coupling of two scalar mesons, σ and δ, and vector ω mesons to scalar δ mesons. In this paper, we extend the model presented in [8] to ω-δ coupling. It is interesting that the model does not include other meson-meson interaction terms, except the very common self-interaction term for the σ meson, but leads to results in complete agreement with the present set of relevant astrophysical observations. For future reference, we name the model Cracow crossing terms (CCT). The total Lagrangian $\mathcal{L}$ leads to the following equations of motion:

$$m_\sigma^2 \bar{\sigma} = g_\sigma \left(n_p^s + n_n^s\right) - U'(\bar{\sigma}) + g_{\sigma\delta} \bar{\sigma} (\bar{\delta}^{(3)})^2, \tag{3}$$

$$m_\omega^2 \bar{\omega}_0 = g_\omega n - g_{\omega\delta} \bar{\omega}_0 (\bar{\delta}^{(3)})^2, \tag{4}$$

$$m_\rho^2 \bar{\rho}_0^{(3)} = \tfrac{1}{2} g_\rho (2x - 1) n, \tag{5}$$

$$m_\delta^2 \bar{\delta}^{(3)} = g_\delta \left(n_p^s - n_n^s\right) + g_{\sigma\delta} \bar{\sigma}^2 \bar{\delta}^{(3)} + g_{\omega\delta} \bar{\omega}_0^2 \bar{\delta}^{(3)}. \tag{6}$$

The meson names with the bars represent the mean field values (for isovector mesons $\vec{\rho}, \vec{\delta}$ only their third component is nonvanishing), n and x are baryon number density and proton fraction $x = n_p/n$, respectively, the scalar densities n_i^s for proton and neutron $i = p, n$ are given by the integrals $n_i^s = \frac{2}{(2\pi)^3} \int_0^{k_{F,i}} \frac{m_i}{\sqrt{k^2 + m_i^2}}\, d^3k$, where $k_{F,i}$ are the nucleon Fermi momenta. The nucleon effective masses m_i, appearing in the integrals do not need to be equal as the nonvanishing $\bar{\delta}^{(3)}$ introduces the effective mass splitting [9]:

$$m_p = m - g_\sigma \bar{\sigma} - g_\delta \bar{\delta}^{(3)}, \tag{7}$$

$$m_n = m - g_\sigma \bar{\sigma} + g_\delta \bar{\delta}^{(3)}. \tag{8}$$

The effective masses can be used to replace the meson mean field of nucleons. Then, after including Eqs. (3)–(8), the energy density for nucleonic matter may be expressed in terms of only the densities and the effective nucleon masses:

$$\begin{aligned} \varepsilon_{\text{nuc}} = {} & \sum_{i=p,n} \frac{1}{4}(3E_{F,i} n_i + m_i n_i^s) + \frac{1}{2C_\sigma^2}(m - \bar{m})^2 \\ & + \frac{C_\omega^2}{2} \frac{n^2}{1 + C_\omega^2 \Lambda_{\omega\delta} (\Delta m/2)^2} + \frac{C_\rho^2}{8}(2x-1)^2 n^2 \\ & + \frac{\Delta m^2}{8C_\delta^2} + \frac{1}{8}\Lambda_{\sigma\delta}(m - \bar{m})^2 \Delta m^2 + U(m - \bar{m}), \end{aligned} \tag{9}$$

where the first term in Eq. (9) represents the energy of the nucleonic Fermi sea, i.e., the integrals $\frac{2}{(2\pi)^3} \int_0^{k_{F,i}} \sqrt{k^2 + m_i^2}\, d^3k$. The integrals can be expressed by already defined scalar densities n_i^s and Fermi energy $E_{F,i} = \sqrt{k_i^2 + m_i^2}$.

The expression for the energy density shows that it is convenient to replace the coupling appearing in the Lagrangian by the following parameters:

$$\begin{aligned} & C_\sigma^2 = \frac{g_\sigma^2}{m_\sigma^2}, \quad C_\omega^2 = \frac{g_\omega^2}{m_\omega^2}, \quad C_\rho^2 = \frac{g_\rho^2}{m_\rho^2}, \quad C_\delta^2 = \frac{g_\delta^2}{m_\delta^2}, \\ \text{and} \quad & \Lambda_{\sigma\delta} = \frac{g_{\sigma\delta}}{g_\sigma^2 g_\delta^2}, \quad \Lambda_{\omega\delta} = \frac{g_{\omega\delta}}{g_\omega^2 g_\delta^2}. \end{aligned} \tag{10}$$

Together with the two constants b and c appearing in the σ self-interaction potential, $U(\sigma) = \frac{1}{3} bm(g_\sigma \sigma)^3 + \frac{1}{4} c(g_\sigma \sigma)^4$, our model possesses eight free parameters: four in the isoscalar sector, C_σ^2, C_ω^2, b, c, and four in the isovector sector, C_ρ^2, C_δ^2, $\Lambda_{\sigma\delta}$, $\Lambda_{\omega\delta}$. These constants cannot be uniquely fitted to the saturation point properties and hence we have some freedom to control the properties of the EoS. One free parameter from the isoscalar sector, C_σ^2, is used to control the stiffness of the EoS and a second from the isovector sector, C_δ^2, controls the symmetry energy behavior.

The isoscalar constants are fitted to the three features: the binding energy per nucleon $E_0 = -16.0$ MeV of symmetric matter at $n_0 = 0.16$ fm^{-3} and its compressibility $K_0 = 230$ MeV. The fourth one, C_σ^2, being a free parameter, takes a value between 12 and 14 fm^2 and ensures that the stiffness of the EoS is sufficient to produce a stellar mass in agreement with observational limits. According to recent observations, the maximum neutron star mass must be above $2.1 M_\odot$, and the adopted values of C_σ^2 allow for such stellar masses.

At the isovector sector, the four constants have to be determined, but only the two saturation point properties are available: the symmetry energy $E_{\text{sym}}(n_0)$ and its slope $L(n_0) = 3n_0 \frac{dE_{\text{sym}}}{dn}$. In the work [8], the σ-δ meson crossing term was introduced and it was shown that it leads to the desired soft symmetry energy. The effects of this term on the neutron star properties were further analyzed in [10]. The model with a σ-δ meson crossing term was also extended to the other meson crossing term, as was done in [11]. However, the effect of $\Lambda_{\sigma\delta}$ on the E_{sym} softening occurs only in the vicinity of the n_0 as the σ meson mean field contributes less to the total energy when the density increases. At higher densities, the vector meson fields are those that contribute more to the total energy. That was our motivation to additionally couple the scalar meson δ to the vector meson ω and test whether such coupling is in agreement with dense matter properties and astrophysical observations. Then the expression for the symmetry energy is

$$E_{\text{sym}}(n) = \frac{1}{8} C_\rho^2 n + \frac{k_0^2}{3E_{F,0}} - C_\delta^2 \frac{m_0^2 n}{2E_{F,0}^2 \left(1 - 3C_\delta^2 \left(\frac{n}{E_{F,0}} - \frac{n_s}{m_0}\right) - C_\delta^2 \Lambda_{\sigma\delta}(m - m_0)^2 - C_\omega^2 \Lambda_{\omega\delta} n^2\right)}, \tag{11}$$

where $E_{F,0}$, m_0, and $n^s = n_p^s + n_n^s$ are the Fermi energy, effective nucleon mass, and scalar density in symmetric matter. By the presence of the two constants $\Lambda_{\sigma\delta}$ and $\Lambda_{\omega\delta}$ in the denominator, one may reduce the slope of the symmetry energy

for a wider range of densities. It would be natural to explore different values of the ω-δ coupling. However, it appears that the model is very sensitive to the value of $\Lambda_{\omega\delta}$. This was already observed in the case of the σ-δ term [8]—tiny changes in the coupling of σ-δ introduced pathologically large changes in the symmetry energy behavior or even lack of solution for equations of motion Eqs. (3)–(6). So, our strategy is to keep the coupling for crossing terms fixed: $\Lambda_{\sigma\delta} = 0.032$,[1] $\Lambda_{\omega\delta} = 0.02$ and the remaining isovector constants C_ρ^2, C_δ^2 are used to obtain the required values of $E_{\rm sym}(n_0)$ and L.

The symmetry energy value at saturation point $E_{\rm sym}(n_0)$ oscillates between 30 and 32 MeV according to recent analysis [7]. There is a correlation between $E_{\rm sym}(n_0)$ and L—the higher $E_{\rm sym}(n_0)$ the higher value of L [7]. As shown in the next section, the lower values of L are preferable, so we adopt the lower $E_{\rm sym}(n_0) = 30$ MeV.

The discrepancies concerning the symmetry energy slope L are much greater. Different nuclear experiments give values spread across a wide range. Those based on the spectral pion ratio suggested $47 < L < 117$ MeV [13]. The most promising experiments based on the measurement of neutron skin, which is correlated with the slope value, give different results. Analysis from PREX-2 (^{208}Pb nucleus) [14,15] suggested $L = 106 \pm 37$ MeV. Including the correlation with parity-violating asymmetry for ^{208}Pb gives $L = 54 \pm 8$ MeV [16]. Experiments with a lighter nucleus, ^{48}Ca, give even smaller values for L. The authors of [17] presented a combined analysis of ^{208}Pb and ^{48}Ca and, in the framework of DFT functionals, were not able to reconcile this discrepancy. They suggested that L is in the range from 15 to 83 MeV. In the work [18], the authors point out that the different results for L come from the fact that different experiments probe the symmetry energy at different densities. Recently, Lattimer [7] extensively discussed the sources of observed discrepancies in the slope measurement and suggested that the most likely value is between 40 and 50 MeV. In view of the above difficulties, we suggest adopting values of L from the range from 40 to 80 MeV.

To sum up, we set up a two-parameter family of nuclear models, described by the C_σ^2 coupling and the value of the slope L. The values of all relevant coupling constants are given in Table I.

TABLE I. Coupling constants for nine CCT models numbered by the values of C_σ^2 and L.

C_σ^2 fm^2	C_ω^2 fm^2	b -	c -	L MeV	C_ρ^2 fm^2	C_δ^2 fm^2
				40	15.2938	2.63799
12	6.9769	0.004733	−0.0052878	60	13.1107	2.24899
				80	9.93091	1.61518
				40	13.9852	2.33674
13	7.9531	0.003695	−0.0045224	60	12.1548	2.02896
				80	9.60636	1.54906
				40	12.9888	2.11461
14	8.9055	0.003005	−0.0039370	60	11.4361	1.86945
				80	9.36054	1.50265

III. RESULTS

The introduced RMF model was used to derive the properties of a spherically symmetric configuration of a neutron star. The β equilibrium applied to dense matter with leptons allows finding the equation of state in the core region, whereas for the crust we applied the Sly4 model [19,20]. For the model with the lowest $L = 40$ MeV, the phase transition occurs and the Maxwell construction was used to describe the phase coexistence. The mass-radius diagram for compact stars is shown in Fig. 1, where the upper panel shows the curves for the full parameter space, characterized by the coupling constant C_σ and the L parameter, which are depicted by various line styles and colors, respectively. The lower panel includes the three chosen curves with $L = 40$ MeV and different C_σ^2 values, and also stellar sequences from other EoSs. Additional EoSs in the lower panel include APR [21], DD2, DD2F [22], BSK20 [23], FSUGarnet, IUFSU, and BigApple [24]. The latter three are similar RMF models to the one we have introduced in this work. In the lower panel, the present compact star measurements and constraints derived from astrophysical observations are shown. Compact star measurements include the observation of the object labelled as HESS J1731-347 that suggests a very compact object of low mass. The blue elliptical regions correspond to NICER measurements of the objects PSR 7040 + 6620 [3] and PSR J0030 + 0451 [4]. The violet dots with associated error bars correspond to the derived radius value from an updated analysis of these objects [3], whereas the orange dot with error bars at 1.4 $M_\odot$ is the result of a Bayesian analysis performed while taking into consideration several compact star measurements [25]. The green and gray regions correspond to the two estimated masses of the components of the binary system that merged and produced gravitational waves in the event GW170817. The upper dashed lines mark a lower-bound interval for the lower component of the event GW190814 under the assumption that it was a rapidly spinning neutron star [26]. Red regions correspond to estimated excluded regions from the analysis of the GW170817 event [27,28].

Figures 2 and 3 show tidal deformability values Λ for compact star sequences. They are derived following the approach introduced in [29]; see [30] for a discussion on the implications for the compact star EoS. Figure 2 shows the dependence of the deformability Λ on the stellar mass M, which obeys the relation $\frac{2}{3} k_2 \frac{R^5}{M5}$, where k_2 is the stellar Love number. The measurement point with associated error bar in the vicinity of the 1.4 $M_\odot$ star is the stellar value estimated from the gravitational wave signal of the neutron star merger GW170817, under the assumption that the neutron stars were slowly spinning [31]. A second estimate from an analysis of the GW190814 event that includes the information from GW170817 [32] is also shown. Figure 3 displays tidal deformability relations for the two stars participating in GW170817. The green regions correspond to the 90% and 50% confidence levels derived from the Bayesian

[1]The value of $\Lambda_{\sigma\delta} = 0.032$ corresponds to the $g_{\sigma\delta} = -0.004$, which was used in [8], in this work we are using a more common convention for names and signs of coupling constants like in [11,12].

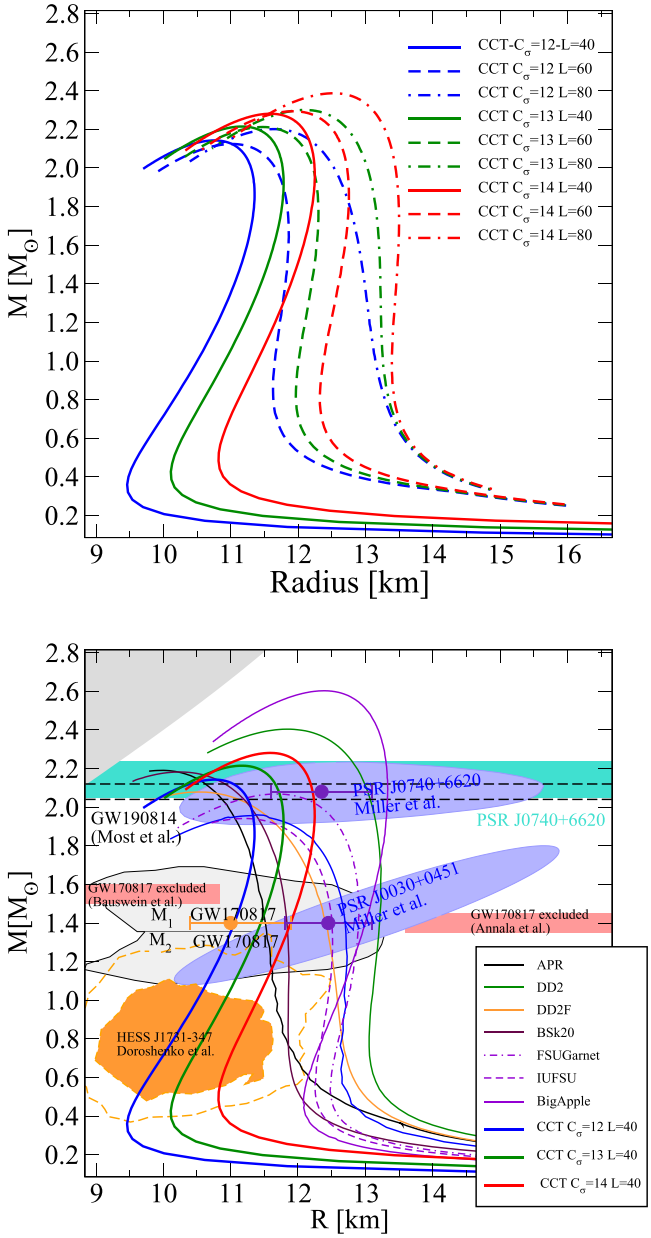

FIG. 1. Mass-radius diagrams of compact stars. The upper panel presents the results for the CCT RMF models introduced in this work, with the Z-like curves obtained for the lowest values of L. The lower panel presents the models with the lowest $L = 40$ MeV and three C_σ^2 values. The curves from other EoS approaches are included. Observational constraints are shown as colored regions and points with error bars; see the text for details.

analysis performed by the LIGO-Virgo collaboration [31]. The general tendency is that more compact stars (which have a lower symmetry energy slope L) agree with this measurement better than larger ones.

IV. CONCLUSIONS AND OUTLOOK

The detection of the compact star associated with the HESS J1731-347 observation has provided a candidate for an ultracompact object of low mass. This measurement represents both a challenge and a strong constraint on EoSs for compact stars. It has already been shown in the reporting article [1] that a set of EoSs derived from chiral perturbation theory as well as strange star models [33] are able to describe such an ultracompact star while simultaneously fulfilling state-of-the-art compact star constraints from other observations.

The article [1] induced hot discussion about dense matter models being able to explain the very compact object. Recent works derived from RMF with density-dependent couplings and tensor forces are barely compatible with HESS J1731-347 [34]. The strange star models proposed in [33,35] and stars with hyperon content [36] are better in describing this measurement. The RMF models with standard couplings seem to be not able to explain lightweight compact star unless

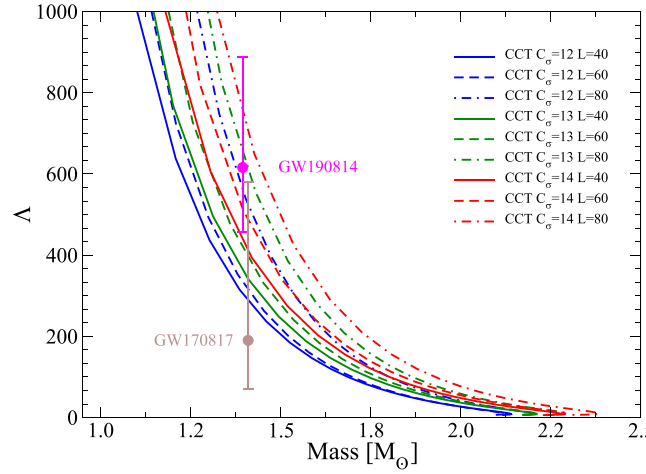

FIG. 2. The tidal deformability as function of neutron star mass. Points with error bars correspond to the star with mass 1.4 $M_\odot$ for the two merger events.

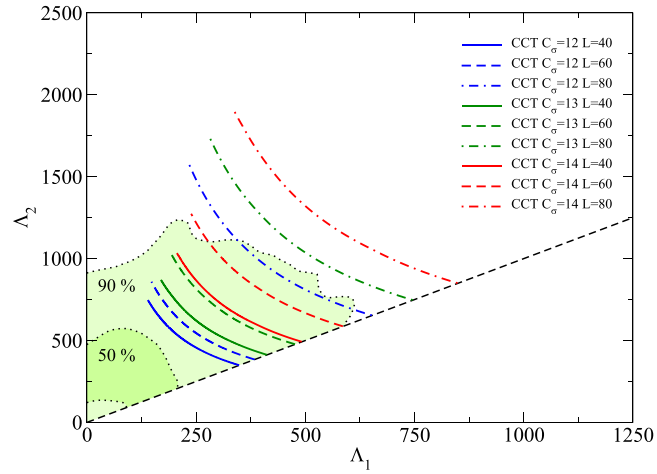

FIG. 3. Tidal deformabilities for two binary components derived from GW170817. RMF models with lower L better fit to the indicated confidence levels.

equipped with exotic component like in [37] where the quark matter core was introduced.

In contrast, in this work we have introduced a purely hadronic RMF with crossing terms among isovector and isoscalar mesons that is able to describe HESS J1731-347 while also reproducing laboratory data such as the saturation properties of nuclear matter. We have found that low values of the symmetry energy slope L, around 40 MeV, for each of the chosen values of the coupling C_σ^2 are best able to reproduce the compact object in HESS J1731-347. The C_σ^2 coupling mainly controls the stiffness of the EoS for more massive stars and the highest value $C_\sigma^2 = 14$ fm^2 seems to be the most preferable in view of the lower bound for maximum mass from precise Shapiro delay measurements for PSR J0740 + 6620.

The higher stiffness of the EoS and the higher C_σ^2 are also supported by the GW events. As can be seen from the measurement shown as a violet dot with associated error bar for the 1.4 $M_\odot$ star in Fig. 1, the coupling $C_\sigma = 14$ fm^2 (red line) is the best value to fulfill this constraint. Furthermore, from the Λ vs. M relation shown in Fig. 2, we can see that the same C_σ value would best fulfill the shared region of Λ for events GW170817 and GW190814, provided the lower mass component in GW190814 is indeed a compact star.

Other properties, such as the cooling features (analyzed in [38]) and rotational configurations of compact stars under the CCT RMF approach presented in this work, are left for a follow-up study.

ACKNOWLEDGMENTS

The authors would like to thank Jorge Piekarewicz for sharing with us a set of equations of state. D.E.A.C. also acknowledges support from the NCN OPUS Project No. 2018/29/B/ST2/02576.

[1] V. Doroshenko, V. Suleimanov, G. Pühlhofer, and A. Santangelo, Nat. Astron. **6**, 1444 (2022).
[2] B. Abbott *et al.* (LIGO Scientific and Virgo Collaboration), Phys. Rev. Lett. **119**, 161101 (2017).
[3] M. C. Miller, F. K. Lamb, A. J. Dittmann, S. Bogdanov, Z. Arzoumanian, K. C. Gendreau, S. Guillot, W. C. G. Ho, J. M. Lattimer, M. Loewenstein *et al.*, Astrophys. J. Lett. **918**, L28 (2021).
[4] M. C. Miller, F. K. Lamb, A. J. Dittmann, S. Bogdanov, Z. Arzoumanian, K. C. Gendreau, S. Guillot, A. K. Harding, W. C. G. Ho, J. M. Lattimer *et al.*, Astrophys. J. Lett. **887**, L24 (2019).
[5] C. A. L. Bailer-Jones, J. Rybizki, M. Fouesneau, M. Demleitner, and R. Andrae, Astron. J. **161**, 147 (2021).
[6] J. A. J. Alford and J. P. Halpern, Astrophys. J. **944**, 36 (2023).
[7] J. M. Lattimer, Particles **6**, 30 (2023).
[8] N. Zabari, S. Kubis, and W. Wójcik, Phys. Rev. C **99**, 035209 (2019).
[9] S. Kubis and M. Kutschera, Phys. Lett. B **399**, 191 (1997).
[10] S. Kubis, W. Wójcik, and N. Zabari, Phys. Rev. C **102**, 065803 (2020).
[11] T. Miyatsu, M. K. Cheoun, and K. Saito, Astrophys. J. **929**, 82 (2022).
[12] B. A. Li, L. W. Chen, and C. M. Ko, Phys. Rep. **464**, 113 (2008).
[13] J. Estee *et al.* (SpiRIT Collaboration), Phys. Rev. Lett. **126**, 162701 (2021).
[14] D. Adhikari *et al.* (PREX Collaboration), Phys. Rev. Lett. **126**, 172502 (2021).
[15] B. T. Reed, F. J. Fattoyev, C. J. Horowitz, and J. Piekarewicz, Phys. Rev. Lett. **126**, 172503 (2021).
[16] P. G. Reinhard, X. Roca-Maza, and W. Nazarewicz, Phys. Rev. Lett. **127**, 232501 (2021).
[17] P. G. Reinhard, X. Roca-Maza, and W. Nazarewicz, Phys. Rev. Lett. **129**, 232501 (2022).
[18] W. G. Lynch and M. B. Tsang, Phys. Lett. B **830**, 137098 (2022).
[19] E. Chabanat, P. Bonche, P. Haensel, J. Meyer, and R. Schaeffer, Nucl. Phys. A **635**, 231 (1998).
[20] F. Douchin and P. Haensel, Astron. Astrophys. **380**, 151 (2001).
[21] A. Akmal, V. R. Pandharipande, and D. G. Ravenhall, Phys. Rev. C **58**, 1804 (1998).
[22] S. Typel, Phys. Rev. C **89**, 064321 (2014).
[23] N. Chamel, A. F. Fantina, J. M. Pearson, and S. Goriely, Phys. Rev. C **84**, 062802(R) (2011).
[24] F. J. Fattoyev, C. J. Horowitz, J. Piekarewicz, and B. Reed, Phys. Rev. C **102**, 065805 (2020).
[25] C. D. Capano, I. Tews, S. M. Brown, B. Margalit, S. De, S. Kumar, D. A. Brown, B. Krishnan, and S. Reddy, Nat. Astron. **4**, 625 (2020).
[26] E. R. Most, L. J. Papenfort, L. R. Weih, and L. Rezzolla, Mon. Not. R. Astron. Soc. **499**, L82 (2020).
[27] A. Bauswein, O. Just, H. T. Janka, and N. Stergioulas, Astrophys. J. Lett. **850**, L34 (2017).
[28] E. Annala, T. Gorda, A. Kurkela, and A. Vuorinen, Phys. Rev. Lett. **120**, 172703 (2018).
[29] T. Hinderer, Astrophys. J. **677**, 1216 (2008).
[30] V. Paschalidis, K. Yagi, D. Alvarez-Castillo, D. B. Blaschke, and A. Sedrakian, Phys. Rev. D **97**, 084038 (2018).
[31] B. P. Abbott *et al.* (LIGO Scientific and Virgo Collaboration), Phys. Rev. Lett. **121**, 161101 (2018).
[32] R. Abbott *et al.* (LIGO Scientific and Virgo Collaboration), Astrophys. J. Lett. **896**, L44 (2020).
[33] F. Di Clemente, A. Drago, and G. Pagliara, arXiv:2211.07485 [astro-ph.HE].
[34] K. Huang, J. Hu, Y. Zhang, and H. Shen, arXiv:2306.04992 [nucl-th].
[35] H. C. Das and L. L. Lopes, MNRAS **525**, 3571 (2023).
[36] J. J. Li and A. Sedrakian, Phys. Lett. B **844**, 138062 (2023).
[37] L. Brodie and A. Haber, Phys. Rev. C **108**, 025806 (2023).
[38] V. Sagun, E. Giangrandi, T. Dietrich, O. Ivanytskyi, R. Negreiros, and C. Providência, arXiv:2306.12326 [astro-ph.HE].